



Influence of cooling water flow rate and temperature on the photovoltaic panel power

Belyamin Belyamin¹ · Mohamad Ali Fulazzaky² · Martin Roestamy² · Rahmat Subarkah¹

¹ Department of Mechanical Engineering, Politeknik Negeri Jakarta, Kampus UI Depok, Depok 16425, Indonesia

² School of Postgraduate Studies, University of Djuanda, Jalan Tol Ciawi No. 1, Ciawi, Bogor 16720, Indonesia

Received: 26 March 2021 / Revised: 22 July 2021 / Accepted: 22 July 2021

© The Joint Center on Global Change and Earth System Science of the University of Maryland and Beijing Normal University 2021

Abstract The photovoltaic panel cooled by a water flowing is commonly used in the study of solar cell to generate the electrical and thermal power outputs of the photovoltaic module. A practical method is therefore required for predicting the distributions of temperature and photovoltaic panel powers over time. In this study, the second-degree polynomial models were established to predict the distributions of temperature and various photovoltaic panel powers, while the linear models were used to analyse the correlation between solar power input and various photovoltaic panel powers. The results showed that the maximum values of electrical power, thermal power and power loss reached at the temperature around noontime. The same value of a photovoltaic panel power recorded at two temperatures was verified from the experiment of photovoltaic panel cooled with different cooling water flow rates. A volumetric flow rate of cooling water passing through the copper tubes determines the amount and characteristics of additional electrical power generated by the water-cooled photovoltaic panel, while a power loss in the photovoltaic panel is very sensitive to the rate of water flow. This study provides a new insight into the management of solar energy for the residential and commercial purposes in the future.

Keywords Electrical power output · Linear regression analysis · Power loss · Second-degree polynomial model · Solar radiation · Thermal power output

List of symbols

a	Correlation coefficient, dimensionless
A	Surface area of the PV panel (m^2)
B	Linear regression constant (W)
C	Specific heat capacity of the water ($\text{J kg}^{-1} \text{K}^{-1}$)
E	Solar irradiation absorbed by the PV panel (W m^{-2})
I	Electrical current produced by the PV panel (A)
m	Mass flow rate of the cooling water (kg s^{-1})
p_o	Polynomial parameter related to temperature ($^{\circ}\text{C}$)
p_1	Polynomial parameter related to temperature ($^{\circ}\text{C h}^{-1}$)
p_2	Polynomial parameter related to temperature ($^{\circ}\text{C h}^{-2}$)
P_{ec}	Electrical power output of the PV panel (W)
P_{in}	Power input to the PV panel (W)
$P_{in(cal)}$	Calculated value of solar power input (W)
P_{loss}	Power loss in the PV panel (W)
$P_{out(cal)}$	Calculated values of either electrical power output, thermal power output, power loss or overall power output (W)
P_{over}	Overall power output of the PV panel (W)
P_{th}	Thermal power output of the PV panel (W)
q_o	Polynomial parameter related to solar irradiation (W m^{-2})
q_1	Polynomial parameter related to solar irradiation ($\text{W m}^{-2} \text{h}^{-1}$)
q_2	Polynomial parameters related to solar irradiation ($\text{W m}^{-2} \text{h}^{-2}$)

✉ Mohamad Ali Fulazzaky
fulazzaky@unida.ac.id; fulazzaky@gmail.com

Belyamin Belyamin
belyamin@yahoo.com

Martin Roestamy
martin.roestamy@unida.ac.id

Rahmat Subarkah
rahmat_subarkah@yahoo.com

r_o	Polynomial parameter related to solar power input (W)
r_1	Polynomial parameter related to solar power input (W h^{-1})
r_2	Polynomial parameter related to solar power input (W h^{-2})
s_o	Polynomial parameter related to electrical power output (W)
s_1	Polynomial parameter related to electrical power output (W h^{-1})
s_2	Polynomial parameter related to electrical power output (W h^{-2})
T	Temperature ($^{\circ}\text{C}$)
t	The time (h)
u_o	Polynomial parameter related to thermal power output (W)
u_1	Polynomial parameter related to thermal power output (W h^{-1})
u_2	Polynomial parameter related to thermal power output (W h^{-2})
V	Electrical voltage produced by the PV panel (V)
v_o	Polynomial parameter related to power loss (W)
v_1	Polynomial parameter related to power loss (W h^{-1})
v_2	Polynomial parameter related to power loss (W h^{-2})
ΔP	Difference between the electrical power output of water-cooled PV panel and the electrical power output of standard PV panel (W)
ΔT	Difference between the inlet and outlet cooling water temperatures of the PV panel (K)

Abbreviations

PV Photovoltaic

PV/T Hybrid photovoltaic/thermal

1 Introduction

Photovoltaic (PV) cell is an electrical device that converts directly the energy of light into electricity by the PV effect. The PV module, which is a packaged connected assembly of the PV cells, can be used as the component of larger PV panel system to generate and supply electricity for the commercial and residential applications. The performance of PV panel is dependent on the environmental factors such as the metrological condition (Daghighi et al. 2011), the availability of solar irradiance at a required location (Zhou et al. 2007), and the PV panel temperature (Skoplaki and Palyvos 2009). An experiment using the hybrid photovoltaic/thermal (PV/T) solar heat pump air-conditioning system has been proposed to deal with the improvement of working conditions of the PV panel by extracting heat from

the PV cells to heat pump working fluid for enhancing operational stability of the panel (Fang et al. 2010). A solar water heating system can either be open loop or closed loop (Jamar et al. 2016). An increase in the water flow rate can lead to a decreased outlet water temperature and increased electrical power output of the PV panel (Mortezapour et al. 2012). A decrease in the operating temperature can boost the open-circuit voltage in a low band gap of the PV semiconductor to enabling a high efficiency of the PV panel (Chen et al. 2009; Dubey et al. 2013). A good choice of the fluid coolant in contact with the PV cells makes it possible to recover the maximum of heat released by Joule effect (Abidi et al. 2014). Water that acts as a working fluid to cool down the PV cells is better than methyl alcohol (Attia and El-Assal 2012) due to the PV panel cooled by a water flowing which can lead to increase the production of electrical current. The water-cooled PV panel collector equipped with a closed-loop oscillating heat pipe has a good performance at the working fluid filling ratios of 60 and 70% with its cooling water flow rates of 9 and 18 L h^{-1} , respectively (Nguyen et al. 2012). A numerical simulation of fluid flow in the wall-mounted hybrid PV/water heating collector system showed that an increase in the working fluid mass flow rate could be beneficial for the PV cooling, leading to an increased electrical and decreased thermal power outputs of the PV panel (Ji et al. 2006).

Using the PV panel can allow a direct conversion of energy from sunlight into electricity (Li et al. 2011; Zhao et al. 2011). The efficiency of PV panel reached higher than 9% depending on the type of the PV cells (Salabaş et al. 2016). More than 80% of solar radiation received by a PV cell are still not converted into electrical power but could be transformed from solar irradiance to thermal power and may cause an increased temperature, leading to a decreased overall performance of solar panel caused by an excessive heat in the PV cells (Dubey et al. 2009). By integrating the PV and solar thermal collector into a building, the PV/T solar system features solar electric and solar thermal technology to harness renewable, free energy from the sun. PV/T collector technology using water as the coolant has an efficiency range of 6–15% (Avezov et al. 2011) and might also have a negative impact in the context of renewable energy sources (Pratiwi and Juerges 2020) and has been seen as a solution to increase the useful power outputs of PV panel. Even if the thermal power efficiency of 58% gained from the typical operating conditions has sufficient capacity for heating water for household use (Chen and Riffat 2011), most PV panels convert around 85% of the sun's energy into heat, which is causing the operating temperature to rise (Li et al. 2002). Using the water-cooled PV panel can increase electrical power and takes advantage of using hot water for residential purpose.

Hot water temperature produced by a water-cooled PV panel can reach 45–50 °C to ensure a sufficient hot water suitable to meet the needs for a residential use (Khordehgah et al. 2020; Sarhaddi et al. 2010). The use of water as cooling fluid could be useful to reduce thermal stress to stabilise the voltage–current characteristics of solar cells with its advantage to extend the service life of PV panel (Ibn-Mohammed et al. 2017).

A number of studies on the water-cooled PV panel technology have been performed since the last three decades (Tyagi et al. 2012). Several models have been proposed to predict the real dynamic or the average performance of PV panel under variable climatic conditions (Hove 2000; Jones and Underwood 2002; Mondol et al. 2005). The electrical power production can be increased by an air cooling system (Tonui and Tripanagnostopoulos 2008). An electrolysis of hydrogen and oxygen from cooling water can increase the performance of PV panel to produce an electrical power due to the PV cells that contain the electric fields force, the free-flowing electrons to flow increasingly with an increase in the cooling water flow rate (Ratlamwala et al. 2011). The performance of PV panel to produce the electrical and thermal powers can be enhanced by a water cooling system (Moharram et al. 2013). The conception of empirical modelling has been associated with several scientific disciplines of using the third-degree polynomial model to predict the accuracy of dawn astronomical twilight (Saksono and Fulazzaky 2020), the quadratic equation to predict the removal efficiency of odorant by the Na_2FeO_4 oxidation (Alibabaei et al. 2021) and the linear regression to predict the value of glycated haemoglobin based on the fasting blood sugar value (Fulazzaky and Fulazzaky 2019). However, the second-degree polynomial models used to predict the distributions of temperature and various PV panel powers observed from the experiment of using different cooling water flow rates are still not fully understood. Correlation of solar power input to PV panel power has not yet been analysed using a linear model. The effect of temperature on the various PV panel powers needs to be verified. Even though the use of water-cooled PV panel could be useful to reduce the temperature of solar cells surface by 10 °C when operated each time for 5 min and to heat around 50 L of water by 40 °C during 5 h of clear sky (Moharram et al. 2013), the effects of water mass flow rate and temperature on the production of various PV panel powers need be verified. Study of the water-cooled PV panel technologies has never been reported before in the context of second-degree polynomial equation used to predict the distributions of temperature and various PV panel powers and also in the context of linear equation used to analyse the correlation between solar power input and various PV panel powers based on the temperature, solar

irradiation, voltage and electrical current data (Ji et al. 2006; Hove 2000; Jones and Underwood 2002; Mondol et al. 2005; Tyagi et al. 2012; Zhou et al. 2007). The polynomial models are commonly considered as an effective and flexible curve fitting technique (Saksono and Fulazzaky 2020). Usually, the polynomial models do not address an underlying functional model and are not based on the theoretical derivations. This study analysed the characteristics of temperature and various PV panel powers using the quadratic equations. The relationship between solar power input and various PV panel powers was analysed using the linear equations. Therefore, the objectives of this study are: (1) to establish the empirical models of quadratic function for use in predicting the distributions of temperature and various PV panel powers over time for the period of 6-h experiment using the PV panel cooled by a water flowing at the rates of 12, 18 and 24 L h⁻¹ and the standard PV panel as reference, (2) to analyse the correlation between two variables, either solar power input and electrical power output, solar power input and thermal power output, solar power input and power loss, or solar power input and overall power output of the PV panel, to gain insights into the contribution of radiant power of the sun to the PV panel power, and (3) to evaluate the effects of cooling water flow rate and temperature on the various PV panel powers, contributed to the current state of knowledge for the next practical application of the PV panels.

2 Materials and methods

2.1 Experimental equipment

This study used (1) one water-cooled PV panel consisting of PV module with its dimension of 0.835-m length × 0.540-m width × 0.028-m height, water storage tank with a capacity of 50 L, copper plate (i.e. roofing copper sheet of ASTM B370 specification with 99% pure copper) and copper tubes (ASTM B88) with an outside diameter of 12.7 mm and (2) one standard PV panel made of the same shape without using a water storage tank as reference for the assessment of electrical power output (see Fig. 1). The type of PV cells used was the multi-crystalline silicon solar cell. For the water-cooled PV panel, the polypropylene pipes fitting shall comply with copper tubes to allow the cooling water flowing into and out of the PV panel. A copper plate coated by the PV cells serves to absorb heat. The PV cells that have a maximum efficiency approximately 12–19% of converting solar energy into electricity are workable for a tolerable heat (Li et al. 2011; Zhao et al. 2011); therefore, the use of copper plate connected with the copper tubes can absorb heat energy from the PV cells. The



Fig. 1 Water-cooled PV panel (left) and standard PV panel (right)

availability of solar thermal energy absorbed by a copper plate and then transferred to the copper tubes can heat the water flowing through the copper tubes of being connected with the polypropylene pipe. Sixteen copper tubes used to circulate the water flow were coated and lagged with a glass wool isolation to reduce the heat loss. The PV cells connected in series have a maximum electrical power of 50 W. The fabricated prototype and experiment setup were performed at the Thermal Engineering Laboratory of the Department of Mechanical Engineering, Politeknik Negeri Jakarta, Depok, Indonesia. The installation of the water-cooled and standard PV panels was directed towards the zenith and oriented slightly facing south (Azimuth 180°), as shown in Fig. 1.

2.2 Experimental procedure and the measurements

Each experiment was carried out at least 6 h to each monitored day of 12 d of the effective experiments. The collection of data during a clear sky of undetected cloud contamination was performed every 15 min from 09:00 to 15:00 h. A substantial efficiency of the PV module is dependent on the weather conditions of approximately 90% originated from a clear sky day (Ando et al. 2020). The measurement of solar irradiation was conducted manually using the portable solarimeter (DELTA OHM DO 9847R, Padova, Italy). The voltage and current generated by the PV panel were recorded using the voltmeter and ammeter (SANWA Digital Multimeter DMM CD772, Tokyo, Japan) connected to the PV module to continuously monitor the voltage and electrical current, respectively, during the experiment. The flow rate of cooling water passing through the circulated water pipe was measured using the graduated cylinder and stopwatch (STOPWATCH-10, Model 20A00D629, Thomas Scientific, Swedesboro, New Jersey,

USA) to ensure the fixed flow rates of 12, 18 or 24 L h⁻¹ aimed at achieving the best possible performance of the PV panel (Nguyen et al. 2012); therefore, the arrangement of intake valve should have a rear water passage to maintain the water flow passed through the copper tubes. To run the experiments of using the water-cooled PV panel at the cooling water flow rates of 12, 18 and 24 L h⁻¹, the circulation of water flow in copper tube was regulated from a storage tank using the peristaltic pump of IPS30 (Espango Peristaltic Pumps Technology, Milano, Italy). The motor power of 75 W used to pump an accurate enough of the cooling water coming from an external source should not affect the calculation of PV panel power in spite of the power generated using a PV water pumping system is more competitive than using a conventional diesel water pumping system (Bouzidi and Campana 2021). The inlet and outlet cooling water temperatures of the PV panel were recorded directly by the data logger of NI-DAQmx 9.0.2 National Instruments (Keysight Electronics Company, Santa Rosa, California, USA).

2.3 Data processing

The water-cooled PV panel should be connected to the copper tubes through which cooling water flows. The PV panel is capable of generating electrical and thermal energy at the same time. The PV panel system used water as the most common coolant to reduce its operating temperature which has the ability to absorb thermal power with heating up water leading to increase the performance of PV panel (Herrando and Markides 2016; Jones and Underwood 2002; Schmidt et al. 2016). The solar power input generated from the sunlight entered the PV cells can be computed using the equation (Idoko et al. 2018; Moharram et al. 2013) of:

$$P_{in} = E \times A \quad (1)$$

The electrical power output of the PV panel can be calculated using the equation (Idoko et al. 2018; Irvine 2017) of:

$$P_{ec} = V \times I \quad (2)$$

The thermal power output of PV panel used to heat water produces a hot water. The thermal power heated the water flowing through a water loop system that can be computed using the equation (Irvine 2017; Moharram et al. 2013) of:

$$P_{th} = m \times C \times \Delta T \quad (3)$$

A second-degree polynomial equation with two roots was used to model the correlation between two random variables (Ostertagová 2012; Smolen and Chuderski 2015) of either T and t , E and t , P_{in} and t , P_{ec} and t , or P_{th} and t , and can be successively written as follows:

$$T = p_0 + p_1t + p_2t^2 \quad (4)$$

$$E = q_0 + q_1t + q_2t^2 \quad (5)$$

$$P_{\text{in}} = r_0 + r_1t + rt^2 \quad (6)$$

$$P_{\text{ec}} = s_0 + s_1t + s_2t^2 \quad (7)$$

$$P_{\text{th}} = u_0 + u_1t + u_2t^2 \quad (8)$$

Fractional power loss is the loss of power that occurs in a PV panel caused by the dissipative effects due to the viscosity, heat conduction and Ohmic losses. There are three main processes of heat transfer: conduction, convection and radiation. The fraction of power loss affected by conduction, convection and radiation can be computed using the equation (Apostolaki-Iosifidou et al. 2017) of:

$$P_{\text{loss}} = P_{\text{in}} - P_{\text{ec}} - P_{\text{th}} \quad (9)$$

A second-degree polynomial equation with two roots was used to model the correlation between two random variables of P_{loss} and t can be written as follows:

$$P_{\text{loss}} = v_0 + v_1t + v_2t^2 \quad (10)$$

The calculated data using Eq. (9) can be used to model the correlation between P_{loss} and t . The overall power output is defined as the sum of electrical and thermal power outputs and power loss, and this can be computed using the equation (Dubey and Tiwari 2009) of:

$$P_{\text{over}} = P_{\text{ec}} + P_{\text{th}} + P_{\text{loss}} \quad (11)$$

A number of models have been proposed to deal with the linear regression analysis, which predicts the value of one continuous variable from another (Fulazzaky 2011; Fulazzaky and Omar 2012). In this work, the linear equation is applicable over a specific limited range of correlation coefficient with the assumptions that (1) any power out of the PV panel can never greater than solar power input to the PV panel and (2) the electrical power output and power loss of the PV panel exist when a solar irradiation has been absorbed by the PV panel. The linear regression analysis was performed to attain a better understanding of the correlation between two power variables, which are the calculated values of either P_{ec} and P_{in} , P_{th} and P_{in} , P_{loss} and P_{in} or P_{over} and P_{in} , using the equation (Fulazzaky and Fulazzaky 2019; Schneider et al. 2010) of:

$$P_{\text{out(cal)}} = aP_{\text{in(cal)}} + b \quad (12)$$

Understanding and analysing a linear correlation between the various types of PV panel power and temperature of the water-cooled PV panel could be helpful for predicting the amounts of solar power input, electrical power output, thermal power output, power loss, and overall power output affected by the operating temperature.

3 Results and discussion

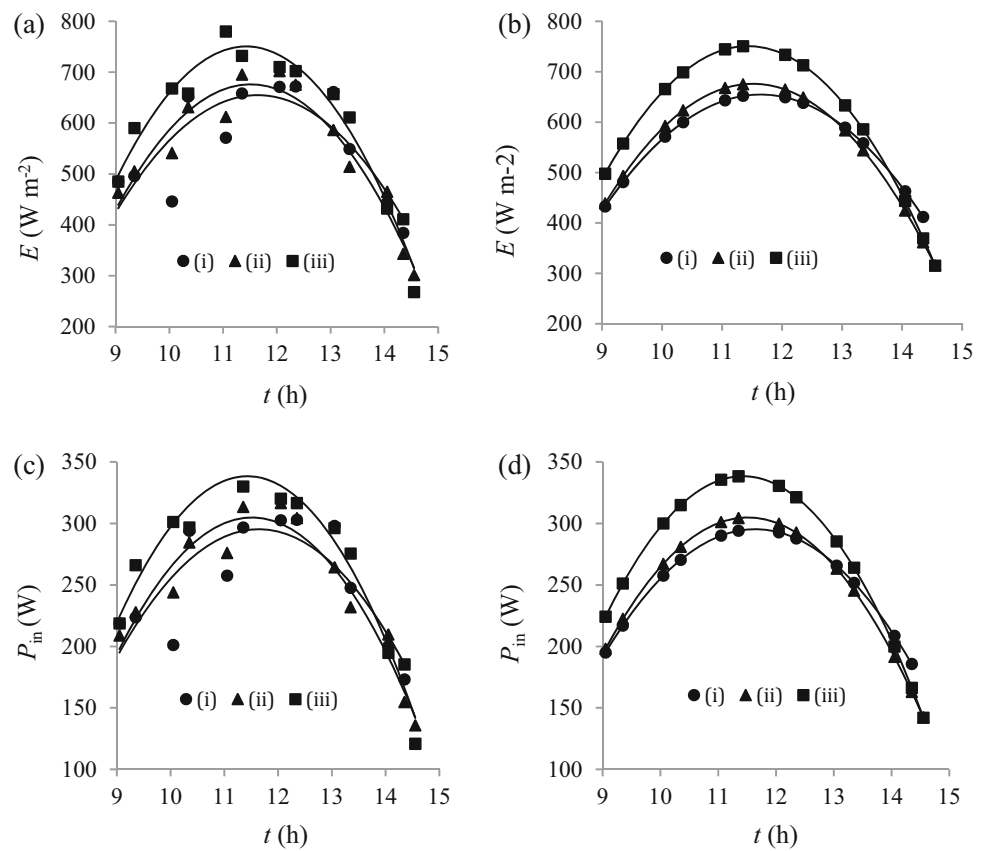
3.1 Solar radiation and power input to the PV panel

The plots (Fig. 2) of E versus t accorded to Eq. (5) and P_{in} versus t accorded to Eq. (6) showing that (1) the variability with an irregular pattern exists in the data of E and P_{in} and (2) the curved graph is concave down, increased from 9:00 h to around noontime and then decreased from around noontime to 15:00 h. The graphs of Fig. 2a, c provide second-order polynomial trendline from a set of data. Test of significance in the functional quadratic regression yields a good fit to the experimental data with R^2 higher than 0.7127 (see Table 1), meaning that the use of the modelled curves of Fig. 2b, d could be useful to predict the distributions of solar radiation intensity and solar power input to the PV panel along the period of 6-h experiment from 9:00 to 15:00 h. The variations of solar irradiation and power input to the PV panel are affected by the weather and depend on the rate of water flowing through a copper tube. According to Eq. (1), the solar power input to the PV panel is directly proportional to the solar radiation intensity for a given surface area of PV panel (Coskun et al. 2011). The charts (Fig. 2b, d) of modelling E or P_{in} versus t show the polynomial fits of order two.

The solar irradiation absorbed by the PV panel varied from 411.9 to 652.1 W m⁻² with an average of 557.4 W m⁻², from 315.7 to 675.0 W m⁻² with an average of 541.1 W m⁻² and from 315.2 to 750.5 W m⁻² with an average of 592.9 W m⁻² can be obtained from a PV panel cooled with the water flow rates of 12, 18 and 24 L h⁻¹, respectively. The increase in peak solar radiation intensity from 652.1 to 675.0 and to 750.5 W m⁻² monitored around noontime can be illustrated by the value of q_0 decreased from - 3832 to - 4502 and to - 5093 W m⁻², the value of q_1 increased from 770.9 to 899.6 and to 1022.5 W m⁻² h⁻¹ or the value of q_2 decreased from - 33.11 to - 39.07 and to - 44.73 W m⁻² h⁻² due to the volumetric flow rate of cooling water increases from 12 to 18 and to 24 L h⁻¹, respectively (see Table 1). Solar radiation reached its maximum intensity along with solar noon could be due to the scattering of sunlight in which scattered photons in the atmosphere have higher photon energy (Joshi et al. 2009; Kostic et al. 2010; Kumar and Tiwari 2010; Shahsavari and Ameri 2010).

The amount of solar energy received on the surface of PV panel varied from 185.7 to 294.0 W with an average of 251.4 W, from 142.3 to 304.3 W with an average of 244.0 W and from 142.0 to 338.3 W with an average of 267.2 W can be obtained from the PV panel cooled by a water flowing at the rates of 12, 18 and 24 L h⁻¹, respectively. The increase in solar energy from 294.0 to

Fig. 2 Curves of E versus t plotted for **a** raw data source and **b** modelled data source and P_{in} versus t plotted for **c** raw data source and **d** modelled data source, based on the data collected from the PV panel cooled with the water flow rates of (i) 12 L h^{-1} , (ii) 18 L h^{-1} and (iii) 24 L h^{-1}



304.3 and to 338.3 W monitored around noontime can be illustrated by the value of r_0 decreased from -1728 to -2030 and to -2296 W , the value of r_1 increased from 347.6 to 405.6 and to 461.0 W h^{-1} or the value of r_2 decreased from -14.93 to -17.62 and to -20.17 W h^{-2} due to the volumetric flow rate of cooling water increases from 12 to 18 and to 24 L h^{-1} , respectively (see Table 1). An increase in solar energy in the PV panel collector reached its maximum value around noontime which could be due to the increase in radiant energy received by the PV cells from the sun (Daut et al. 2012). The modelled curves (see Fig. 2b, d) of E versus t and P_{in} versus t show relatively in good agreement with the experimental data regarding the peak positions and graphs of second-degree polynomials. The graphs of line-(i) and line-(ii) in Fig. 2b, d are almost similar to each other where these two curved lines pass through almost all the points below the graph of line-(iii). This indicates that the radiant energy received by the PV cells from the sun for an experiment of the PV panel cooled by a water flow rate of 24 L h^{-1} is obviously higher than that cooled by the water flow rates of 12 and 18 L h^{-1} due to the cooling of PV panel starts when the temperature of PV panel reaches a maximum allowable temperature of 45°C (Moharram et al. 2013).

3.2 Temperature of the PV panel

The plots (Fig. 3a, c, e) of T versus t according to Eq. (4) yielding second-degree polynomial trendline have a good fit to the experimental data with R^2 higher than 0.6904 (see Table 2). A quadratic regression line of Fig. 3a has the forms of second-degree function in Fig. 3a line-(i) with $R^2 = 0.69045$ observed from the water-cooled PV panel and in Fig. 3a line-(ii) with $R^2 = 0.71956$ observed from the standard PV panel (see Table 2). A quadratic regression line of Fig. 3c has the forms of second-degree function in Fig. 3c line-(i) with $R^2 = 0.71075$ observed from the water-cooled PV panel and in Fig. 3c line-(ii) with $R^2 = 0.86275$ observed from the standard PV panel (see Table 2). A quadratic regression line of Fig. 3e has the forms of second-degree function in Fig. 3e line-(i) with $R^2 = 0.70158$ observed from the water-cooled PV panel and in Fig. 3e line-(ii) with $R^2 = 0.83174$ observed from the standard PV panel (see Table 2). The use of these quadratic equations could be a useful tool to estimate the operating temperature of the water-cooled and standard PV devices, depending on the amount of solar irradiation received by the surface of PV panels. An analysis of the calculated operating temperature data can be used to describe the effect of different water flow rates on the

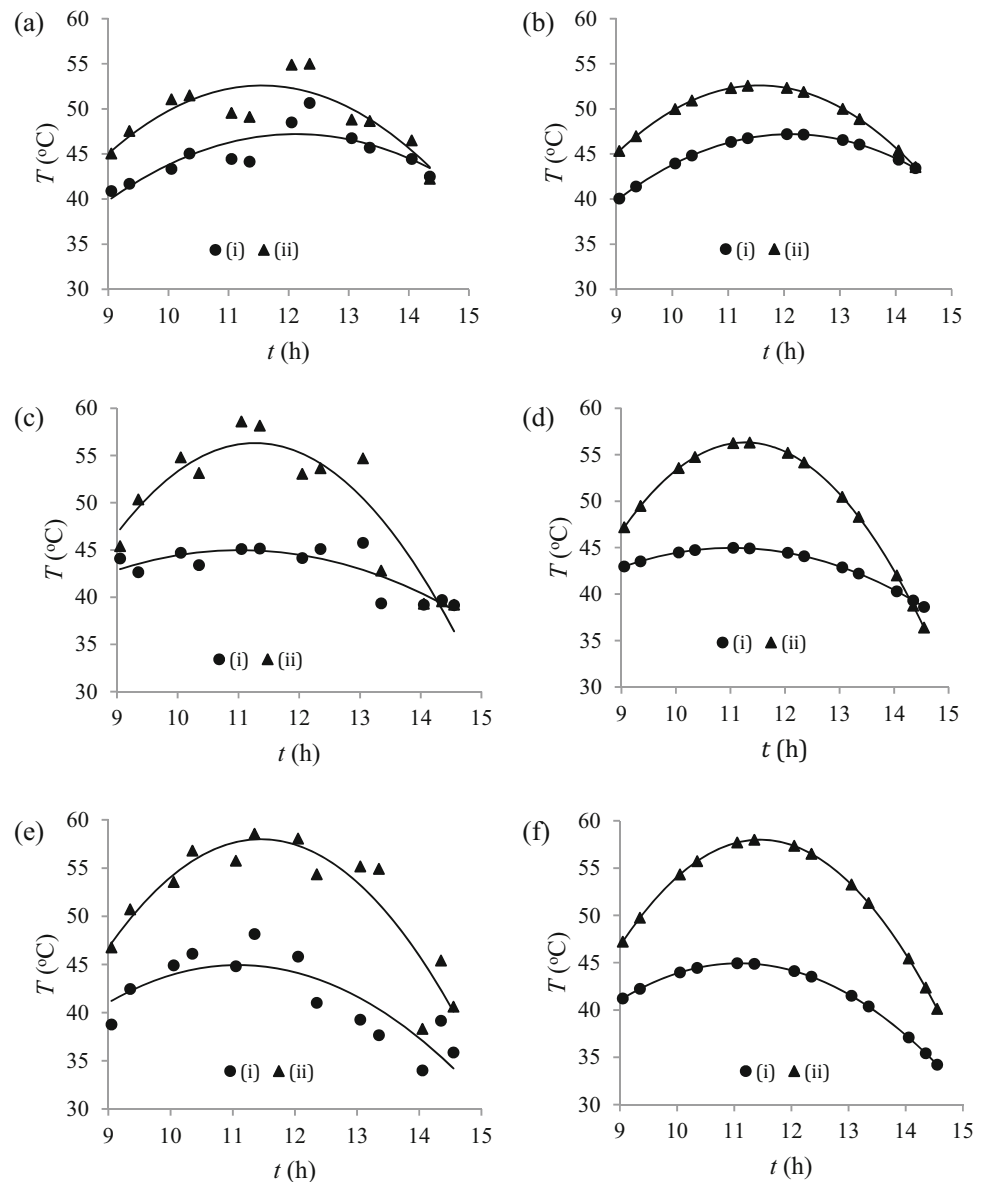
Table 1 Regression analysis of second-degree polynomial model for the solar radiation and various PV panel powers

Q (L h ⁻¹)	Values of the parameters in equation of: $E = q_0 + q_1 t + q_2 t^2$			R^2
	q_2 (W m ⁻² h ⁻²)	q_1 (W m ⁻² h ⁻¹)	q_0 (W m ⁻²)	
<i>Solar radiation</i>				
12	− 33.11	770.9	− 3832	0.71277
18	− 39.07	899.6	− 4502	0.93741
24	− 44.73	1022.5	− 5093	0.96129
Values of the parameters in equation of $P_{in} = r_0 + r_1 t + r_2 t^2$				
	r_2 (W h ⁻²)	r_1 (W h ⁻¹)	r_0 (W)	
<i>Power input to the PV cells</i>				
12	− 14.93	347.6	− 1728	0.71277
18	− 17.62	405.6	− 2030	0.93741
24	− 20.17	461.0	− 2296	0.96129
Values of the parameters in equation of $P_{ec} = s_0 + s_1 t + s_2 t^2$				
	s_2 (W h ⁻²)	s_1 (W h ⁻¹)	s_0 (W)	
<i>Electrical power output of the water-cooled PV panel</i>				
12	− 2.61	60.1	− 291	0.87898
18	− 2.65	60.2	− 289	0.93458
24	− 3.84	88.4	− 446	0.93221
Values of the parameters in equation of $P_{ec} = s_0 + s_1 t + s_2 t^2$				
	s_2 (W h ⁻²)	s_1 (W h ⁻¹)	s_0 (W)	
<i>Electrical power output of the standard PV panel</i>				
12	− 2.89	66.0	− 328	0.86349
18	− 2.64	60.3	− 296	0.95748
24	− 3.66	84.4	− 430	0.91648
Values of the parameters in equation of $P_{th} = u_0 + u_1 t + u_2 t^2$				
	u_2 (W h ⁻²)	u_1 (W h ⁻¹)	u_0 (W)	
<i>Thermal power output of the water-cooled PV panel</i>				
12	− 9.18	215.8	− 1093	0.75856
18	− 11.71	263.9	− 1299	0.63803
24	− 11.64	265.9	− 1338	0.79315
Values of the parameters in equation of $P_{loss} = v_0 + v_1 t + v_2 t^2$				
	v_2 (W h ⁻²)	v_1 (W h ⁻¹)	v_0 (W)	
<i>Power loss in the water-cooled PV panel</i>				
12	− 3.14	71.7	− 343	1.00000
18	− 3.26	81.5	− 443	1.00000
24	− 4.69	106.7	− 513	1.00000
Remarks that Q means the volumic flow rate of cooling water				

temperature of PV panel by plotting T versus t , as shown in Fig. 3b, d, f. A set of 12 L h⁻¹ for specifying the minimum flow rate, at which the hydraulic interactions cause a force which may probably compromise the laminar flow, can reduce the temperature of PV panel varied from 0.1 to 6.1 °C with an average of 4.3 °C (see Fig. 3b). A set of

18 L h⁻¹ for specifying the moderate flow rate, at which the hydraulic interactions cause a force which may probably compromise a mix of the laminar and turbulent flows, can reduce the temperature of PV panel varied from -2.2 to 11.4 °C with an average of 6.6 °C (see Fig. 3d). A set of 24 L h⁻¹ for specifying the maximum flow rate, at which

Fig. 3 Curves of T versus t plotted for firstly **a** raw data source and **b** modelled data source in the case of given a volumetric water flow rate of 12 L h^{-1} , secondly **c** raw data source and **d** modelled data source in the case of given a volumetric water flow rate of 18 L h^{-1} , and thirdly **e** raw data source and **f** modelled data source in the case of given a volumetric water flow rate of 24 L h^{-1} , with (i) the water-cooled PV panel and (ii) the standard PV panel



the hydraulic interactions cause a force which may probably compromise the turbulent flow, can reduce the temperature of PV panel varied from 5.9 to 13.2 °C with an average of 10.1 °C (see Fig. 3f). A high mass flow rate of cooling water-enhanced reduction in operating temperature can help improve the performance of PV panel (Coskun et al. 2011; Moharram et al. 2013).

3.3 Electrical power output of the PV panel

The plots (Fig. 4a, c) of P_{ec} versus t accorded to Eq. (7) yielding the graph of quadratic function provide a good fit to the experimental data with R^2 higher than 0.8634 (see Table 1). The curved lines of Fig. 4b, d are only valid for clear sky of tropical regions caused by the meteorological

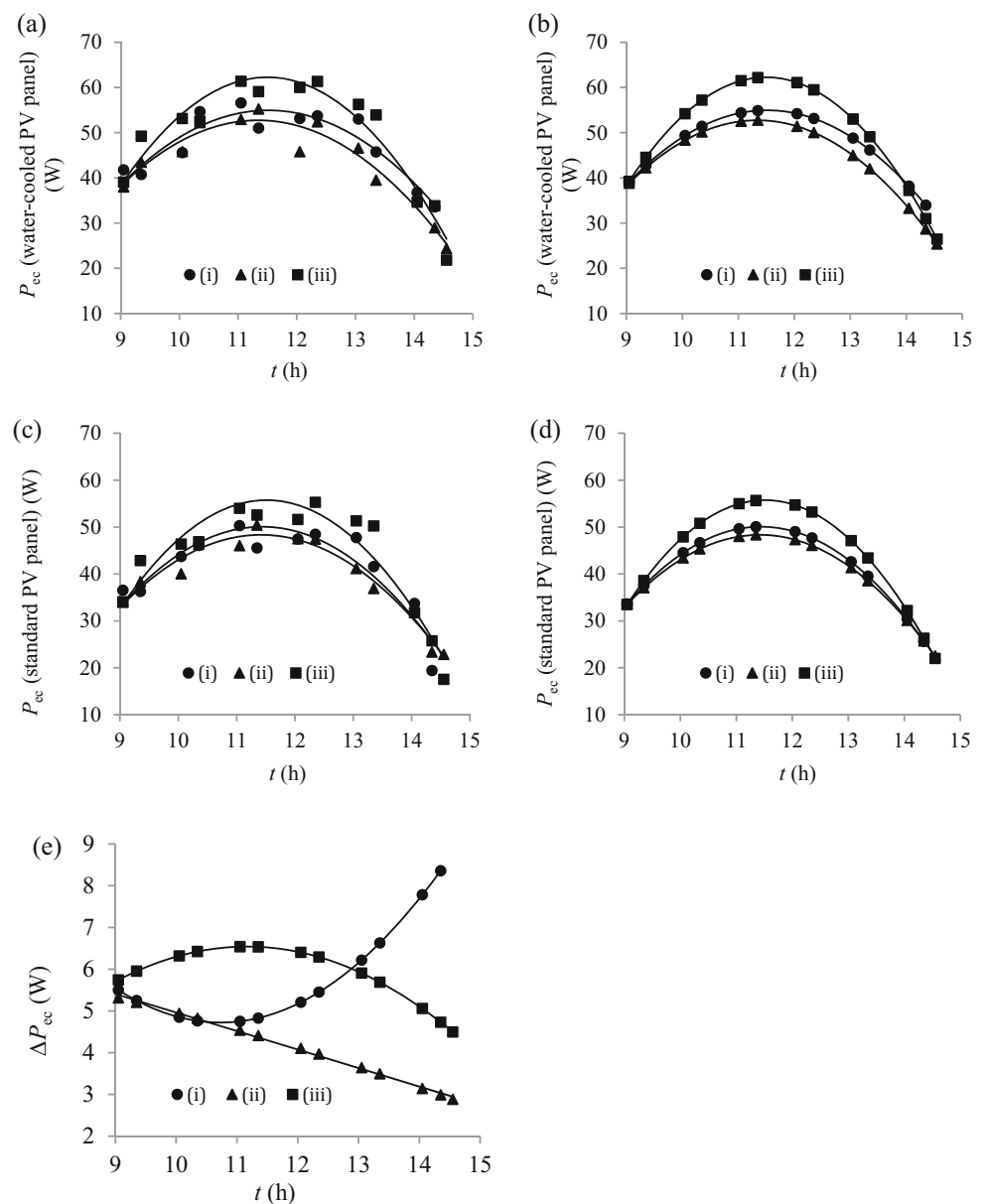
conditions affecting electrical power output of the PV panel, meaning that the use of modelled curves in Fig. 4b, d could be useful to predict the distribution of electrical power observed from the water-cooled and standard PV panels along the experimental period of 6-h from 9:00 to 15:00 h. The PV panel cooled by a water flowing can produce more electrical current compared to the standard PV panel without incorporated a cooling water flow as shown by the variations of the P_{ec} values in Fig. 4b at all the pairs of points higher than those in Fig. 4d accordingly. The electrical power varies from 34.0 to 54.9 W with an average of 47.2 W, from 25.4 to 52.7 W with an average of 43.1 W and from 26.5 to 62.2 W with an average of 48.9 W observed from the PV panel cooled by a water flowing at the rates of 12 , 18 and 24 L h^{-1} , respectively

Table 2 Regression analysis of the second-degree polynomial models plotted for the operating temperature data of the water-cooled and standard PV panels

Q (L h ⁻¹)	Values of the parameters in equation of $T = p_0 + p_1 t + p_2 t^2$			
	p_2 (°C h ⁻²)	p_1 (°C h ⁻¹)	p_0 (°C)	R^2
<i>A plot of T versus t for data collected from the water-cooled PV panel</i>				
12	- 0.758	18.38	- 64.2	0.69045
18	- 0.513	11.32	- 17.4	0.71075
24	- 0.895	19.85	- 65.1	0.70158
<i>A plot of T versus t for data collected from the standard PV panel</i>				
12	- 1.159	26.79	- 102.2	0.71956
18	- 1.853	41.77	- 179.1	0.86275
24	- 1.867	42.76	- 186.9	0.83174

Remarks that Q means the volumic flow rate of cooling water

Fig. 4 Curves of P_{ec} versus t plotted for firstly **a** raw data source and **b** modelled data source observed from the water-cooled PV panel, secondly **c** raw data source and **d** modelled data source observed from the standard PV panel, and thirdly **e** the curves of plotting ΔP_{ec} versus t , with the water flow rates of (i) 12 L h⁻¹, (ii) 18 L h⁻¹ and (iii) 24 L h⁻¹



(see Fig. 4a). The electrical power varies from 25.6 to 50.1 W with an average of 41.4 W, from 22.5 to 48.3 W with an average of 39.0 W and from 22.0 to 55.6 W with an average of 43.1 W observed from the standard PV panel monitored in parallel with the monitoring of water-cooled PV panel observed at the water flow rates of 12, 18 and 24 L h⁻¹, respectively (see Fig. 4c). The average electrical power varied from 47.2 to 43.1 and to 48.9 W observed from the water-cooled PV panel and from 41.4 to 39.0 and to 43.1 W observed from the standard PV panel could be due to the flow rate of cooling water increases from 12 to 18 and to 24 L h⁻¹, respectively (see Fig. 4a, c). A change in the daily weather and normal temperature of the tropical region can lead to a change in the production of electrical power as shown by the graphs in line-(ii) of Fig. 4b, d. The effect of water flow rate increased from 12 to 18 and to 24 L h⁻¹ on the electrical power production can lead to an increased maximum value of electrical power from 9.5% to 9.1% and to 11.9%, respectively. The electrical power production by a water-cooled PV panel could be proportional to an input of the radiant energy, which can reach a maximum value at around noon, due to the altitude of the sun varies throughout the day of clear sky and reaches its less cosine loss at around noontime.

A plot (Fig. 4e) of ΔP_{ec} versus t yielding (1) the second-degree polynomial equation with $R^2 = 1.0000$ observed from the PV panel cooled by a water flow rate of 12 L h⁻¹, (2) the linear equation with $R^2 = 0.99713$ observed from the PV panel cooled by a water flow rate of 18 L h⁻¹ and (3) the second-degree polynomial equation with $R^2 = 1.0000$ observed from the PV panel cooled at by a water flow rate of 24 L h⁻¹ can be successively written as:

$$\Delta P_{ec} = 0.277t^2 - 5.95t + 36.6 \quad (13)$$

$$\Delta P_{ec} = -0.443t + 9.40 \quad (14)$$

$$\Delta P_{ec} = -0.179t^2 + 3.99t - 15.7 \quad (15)$$

The graph of second-degree polynomial in line-(i) of Fig. 4e showing an additional electrical power of ΔP_{ec} gradually decreases to reach its lower value of 4.8 W around noontime and then increases with an increase in time t . The linear trendline in line-(ii) of Fig. 4e showing an additional electrical power of ΔP_{ec} continuously decreases with an increase in time t . The graph of second-degree polynomial in line-(iii) of Fig. 4e showing an additional electrical power of ΔP_{ec} gradually increases to reach its higher value of 6.5 W (peak) around noontime due to the dynamic model of thermal absorber powered by a solar irradiance which leads to an increased additional electrical power (Allouhi et al. 2014) and then decreases with an increase in time t . Empirical evidence shows that additional electrical power of ΔP_{ec} delivered from the PV panel is highly affected by the water flow passed through

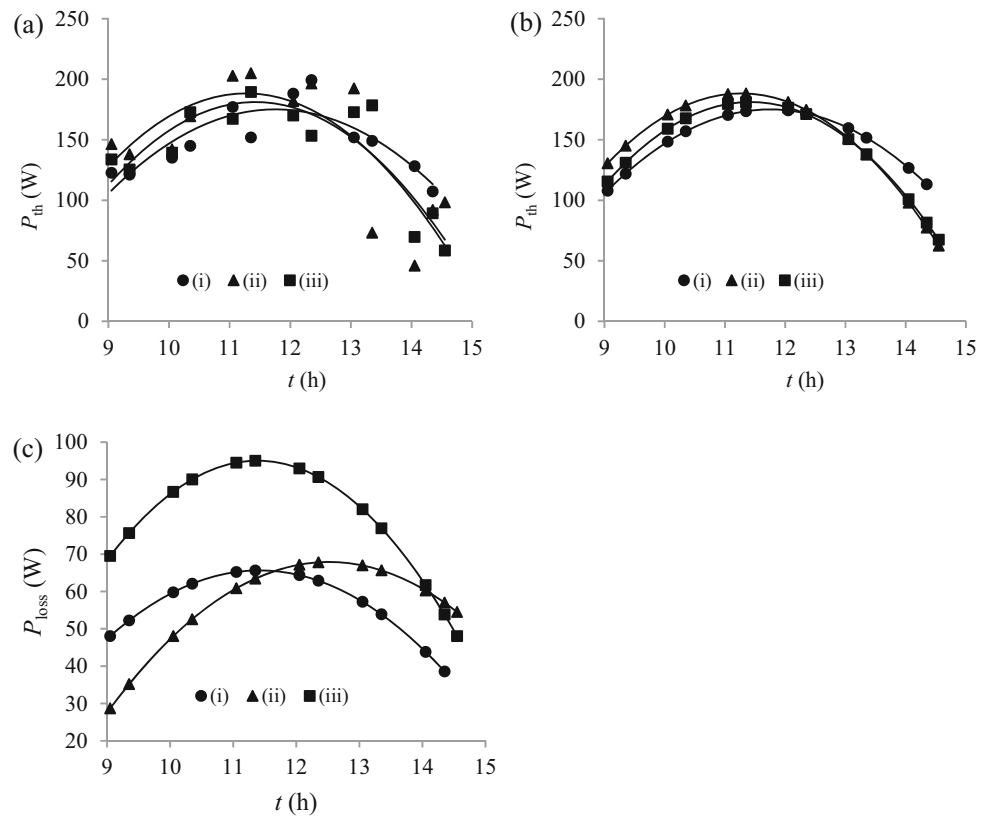
the copper tubes and depends on the solar irradiation reaching the PV cells (Maghami et al. 2016). For long-time application, the PV panel cooled by a water flow rate of 12 L h⁻¹ is better than increased stability of additional electrical power production, as shown in the line-(i) of Fig. 4e.

3.4 Thermal power output of the PV panel

The advantages of water cooling over air cooling include the distinctive characteristics of water showed with its higher specific heat capacity, density and thermal conductivity (Zimmermann et al. 2012). In this work, the PV panel cooled by a water flow rate passing through the copper tubes of being connected with copper plate absorber was used as the experimental tool to achieve one of the attainable goals in understanding the distribution pattern of thermal power along the period of 6-h experiment (see Fig. 5a, b). Understanding of the thermal power distribution gains an insight into the production of electrical power and useful life of the PV panel. Using solar energy to heat an amount of water for the commercial and residential applications could be one of the most practical and cost-effective ways to harness energy from the sun.

A plot (Fig. 5a) of P_{th} versus t providing graph of quadratic function represents a moderate fit to the experimental data (with $R^2 > 0.6380$; see Table 1). Therefore, the use of modelled curves in Fig. 5b could be useful to predict the distribution of thermal power generated by a PV panel along the experimental period of 6 h from 9:00 to 15:00 h. Figure 5b shows that the thermal power varied from 107.9 to 173.5 W with an average of 148.0 W, from 62.5 to 188.2 W with an average of 144.8 W and from 67.4 to 181.1 W with an average of 140.0 W can be obtained from the experiments of PV panel cooled by the water flow rates of 12, 18 and 24 L h⁻¹, respectively. The average thermal power decreased from 148.0 to 144.8 and to 140.0 W could be due to an increased flow rate of the cooling water from 12 to 18 and to 24 L h⁻¹. An increased rate of water flow that passed through the copper tubes can lead to an increase in the heat released from the PV cells affecting the thermal power output of PV panel decreases. The effect of increased water flow rate on the lifetime of stimulated and spontaneous emission in a semiconductor device can reduce the operating temperature and improves the performance of PV module caused by the prolonged exposure to a low temperature. Because the penetration of radiation over most of the useful spectra is extremely shallow, the copper tubes must be placed as near to the PV panel surface as possible (Chaplin et al. 1954). An attempt to use the panel of PV conditioned at cooler temperature is really better than hot ones due to the average thermal power

Fig. 5 Curves of P_{th} versus t plotted for **a** raw data source and **b** modelled data source, while **c** the curves of P_{loss} versus t , based on the data observed from the PV panel cooled with the water flow rates of (i) 12 L h^{-1} , (ii) 18 L h^{-1} and (iii) 24 L h^{-1}



which decreases with an increase in the cooling water flow rate, which leads to a decreased operating temperature.

3.5 Power loss in the PV panel

A plot (Fig. 5c) of P_{loss} versus t providing graph of quadratic function represents an excellent fit to the calculated data (with $R^2 = 1.0000$; see Table 1). The loss of PV power varied from 38.6 to 65.6 W with an average of 56.2 W, from 28.7 to 67.8 W with an average of 56.0 W and from 48.1 to 95.0 W with an average of 78.3 W can be obtained from the experiment using the panel of PV cooled by the water flow rates of 12, 18 and 24 L h^{-1} , respectively (see Fig. 5c). The maximum power loss of 65.6 W recorded at 11:35 h and 67.8 W at 12:35 h of the experimental day can be verified from the second-degree polynomial graphs of line-(i) and line-(ii), respectively, in Fig. 5c and are almost similar to each other compared to the maximum power loss of 95.0 W recorded at 11:35 h from the polynomial graph of line-(iii) in Fig. 5c. Even though the power loss varying over time is dependent on the irradiation of solar received by the PV panel, the level of power loss in a PV panel can be optimised by an arrangement of water flowing through the copper tubes by using a fixed flow rate of cooling water passed through the copper tubes. Empirical evidence (Fig. 5c) shows that the PV panel cooled by a

water flow at the rates of 12 and 18 L h^{-1} can help minimise the loss of power by 44.8% and 40.1%, respectively, compared to that cooled by a water flow rate of 24 L h^{-1} . Using the water-cooled PV panel can provide the opportunity for having the comparable environmental and energy benefits with regard to the commercial and residential applications (Carnevale et al. 2014). The implication of water used to cool the PV panel could be helpful in reducing the thermal stress and stabilises the voltage–current characteristics of PV cells causing the useful life of PV panel increases. In spite of the flow rate of cooling water passing through the copper tubes determines a trend of power loss, the loss of power in PV panel is dependent on the irradiance, temperature and amount of current drawn from the PV panel.

3.6 Correlation of solar power input to the various PV panel powers

By plotting the correlation between various PV panel powers and solar power input accorded to Eq. (12), yielding the graphs of linear function reveals a very good fit to the calculated data with R^2 higher than 0.9199, except one graph of nonlinear function to correlate the power loss with solar power input for the experiment of using the panel of PV cooled by a water flow rate of 18 L h^{-1} (see

Fig. 6; see also Table 3). The results (Fig. 6a–d) show that an increase in the solar power input can lead to an increased power of the PV panel, which could naturally be higher at a higher light intensity level (Katz et al. 2001). Experimental evidence of Fig. 6a shows that (1) the average values of electrical power are as high as 47.2, 43.1 and 48.9 W observed from a PV panel cooled by the water flow rates of 12, 18 and 24 L h⁻¹, respectively, and (2) the increasing trends of three linear regression lines are close to each other. For the graphs of linear function in lines-(i, ii, iii) of Fig. 6a, an increase in the electrical power with the increasing in the solar power input looks almost similar to each other, which indicates a change in the cooling water flow rate which does not affect a significant change of the trend in electrical power generated by the PV panel.

The average value of thermal power which decreased from 148.0 to 144.0 and to 140.0 W was observed from the experiments of using the panel of PV cooled by the rate of water flow increased from 12 to 18 and to 24 L h⁻¹, respectively (see Fig. 6b). An increase in the cooling water flow rate from 12 to 18 L h⁻¹ and from 12 to 24 L h⁻¹ may lead to cause the generation of thermal power decreased by 2.7% and 5.4%, respectively. The line-(iii) of Fig. 6b shows a separate trendline in each point of the charts to visualising the panel of PV cooled by a water flow rate of 24 L h⁻¹. The implication of using a water-cooled

PV panel to harvest the sun's energy can decrease the thermal power of PV module due to the heat absorbed by a water flow which increases with an increase in the water flowing through the copper tubes. Most fraction of incoming solar irradiation received by the PV panel is converted to thermal power for heating the circulated cooling water. The development of conceptual models of PV module offers affordable, renewable energy plans for the commercial and residential hot water applications (Alshuraiaan 2021). Even though many physical models of the PV panel have been proposed to generate electrical power (Kalogirou and Tripanagnostopoulos 2006), the development of water-cooled PV panel generated an additional thermal power could be cost effective if the additional cost of thermal unit used is low. Long residence time of water flowing through the copper tubes could pick up more heat. Circulating the water in the copper tubes can have an increased chance to absorb heat more since the flow rate of cooling water is slow. Cooling water that having a high specific heat can absorb a large amount of heat energy. An innovative solar water heating system can be proposed as the renewable energy heat source for the commercial and residential purposes after analysing cost-benefits to find out the limits of its practical uses in the future. Both the electrical and thermal conductions in copper occur mainly via the free electrons, while the

Fig. 6 Curves of plotting **a** P_{ec} versus P_{in} , **b** P_{th} versus P_{in} , **c** P_{loss} versus P_{in} and **d** P_{over} versus P_{in} for the experiments of using the panel of PV cooled with the volumetric water flow rates of (i) 12 L h⁻¹, (ii) 18 L h⁻¹ and (iii) 24 L h⁻¹

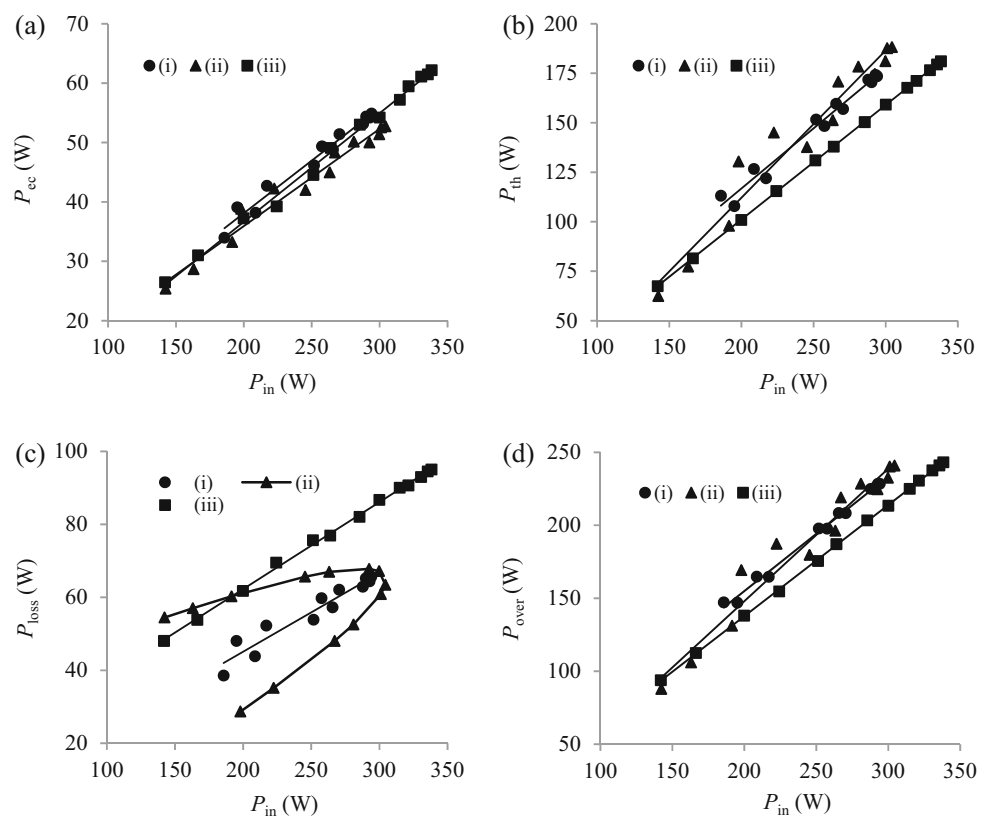


Table 3 Linear regression analysis of plotting the curves of various PV panel powers versus solar power input

Q (L h ⁻¹)	Values of the parameters in equation of $P_{\text{out(cal)}} = a P_{\text{in(cal)}} + b$		
	a (dimensionless)	b (W)	R^2
<i>Correlation between electrical power and power input</i>			
12	0.1771	2.6771	0.97276
18	0.1637	3.1773	0.97051
24	0.1831	0.0185	0.99493
<i>Correlation between thermal power and power input</i>			
12	0.6074	− 4.6619	0.97700
18	0.7444	− 36.7660	0.94783
24	0.5786	− 14.6210	0.99998
<i>Correlation between power loss and power input</i>			
12	0.2155	1.9849	0.91994
18	–	–	–
24	0.2383	14.6030	0.99810
<i>Correlation between overall power output and power input</i>			
12	0.7845	− 1.9849	0.99348
18	0.9081	− 33.5890	0.95233
24	0.7617	− 14.6020	0.99981

Remarks that Q means the volumic flow rate of cooling water

relationship between electrical and thermal conductance can be described by the Wiedemann–Franz law based on the fact that the electrical and heat transports involve the free electrons in a copper (Bangura et al. 2013; Lin et al. 2014; Wang et al. 2013). The use of water cooling coolant can reduce the operating temperature of PV module and can improve the internal photoelectric effect causing an increase in the electrical power due to the function of absorber material inside the copper plate collector which is to convert the sunlight to heat energy and then to heat the cooling water in the copper tubes.

A change in the cooling water flow rate may cause a very significant change of the power loss shown by a separate straight line graph of two linear functions in the lines-(i, iii) of Fig. 6c observed from the experiments of using the panel of PV cooled by the water flow rates of 12 and 24 L h⁻¹, respectively, and by one graph of nonlinear function in the line-(ii) of Fig. 6c observed from the panel of PV cooled by a cooling water flow rate of 18 L h⁻¹. A water spray cooling method of comparing the different spray angles has been investigated to enhance the performance of PV panels (Nateqi et al. 2021). The key feature of linear and nonlinear functions could be due to the dependent variable changes at a constant and nonconstant rate with the independent variable. The graph of power loss as a function of solar power input is dependent on the characteristics of water flowing through the copper tubes. The average power loss of 56.2 W observed from the panel of PV cooled by a water flowing at the rate of 12 L h⁻¹ is very close to that of 56.0 W observed from the panel of PV

cooled by a water flow rate of 18 L h⁻¹. However, the average power loss of 78.3 W caused by the effects of conduction, convection and radiation observed from the panel of PV cooled by a water flow rate of 24 L h⁻¹ is possible to produce more than 39% (> 22 W) of the power loss compared to those observed from the water-cooled PV panel flowed a water through the copper tubes at the rates of 12 and 18 L h⁻¹. A different trend in the lines-(i, ii, iii) of Fig. 6c could be dependent on the characteristics of water flow passed through the copper tubes, which can determine the amount of power loss in a PV panel.

Figure 6d shows that the average values of overall power output are as high as 195.2, 187.9 and 188.9 W observed from the panel of PV cooled by a water flowing at the rates of 12, 18 and 24 L h⁻¹, respectively. The linear curves of P_{over} versus P_{in} (see Fig. 6d) looked very similar to those of P_{th} versus P_{in} (see Fig. 6b) which could be due to the average thermal power of around 145 W that dominantly contributes to the average value of overall power output of around 190 W. The efficiency of overall power output generated by a PV panel can reach at its maximum with an approximate temperature in the range of 47–60 °C (Katz et al. 2001). At such a temperature range, the mobilised electrons are characterised by the most effective temperatures and very mobile likely to leave the PV cells even though the mobility of electrons in semiconductor caused a recombination which can lead to a decreased electrical power at the temperatures of greater than 60 °C. At an appropriate temperature, the net solar energy transferred to a water-cooled PV panel can allow to increase the

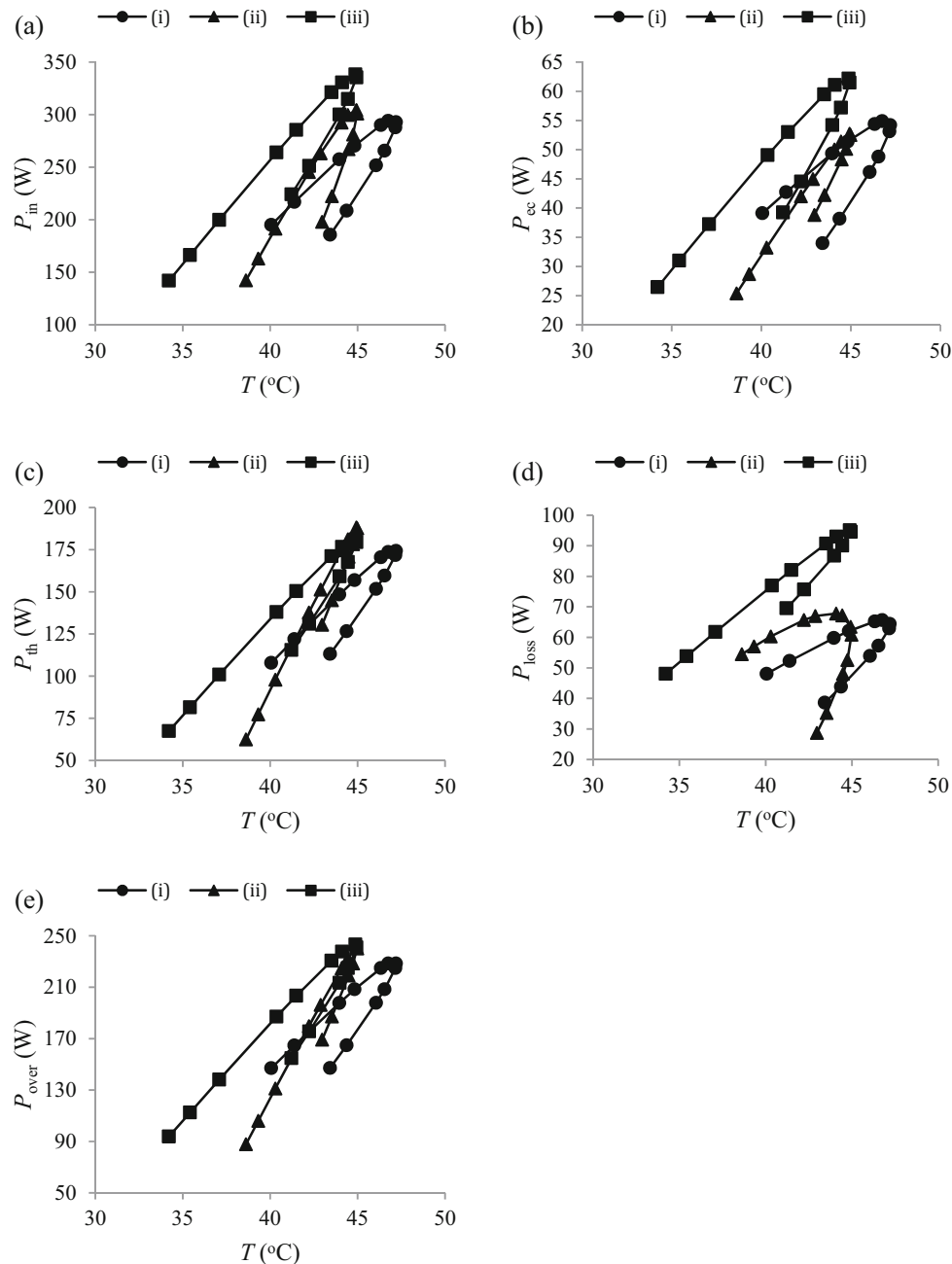


Fig. 7 Curves of plotting **a** P_{in} versus T , **b** P_{ec} versus T , **c** P_{th} versus T , **d** P_{loss} versus T and **e** P_{over} versus T based on the data monitored from the panel of PV cooled with the water flow rates of (i) 12 L h^{-1} , (ii) 18 L h^{-1} and (iii) 24 L h^{-1}

momentum of the mobile electrons, holes and lattice cell holes. Lattice relaxation of PV panel can shift an equilibrium position of the lattice atoms and arises from an interaction between the electrons and the lattices (Wang and Li 2012). In this work, the maximum efficiency of overall power output reached approximately 92.6% that can be maintained at a PV panel temperature of 45.1°C , which is lower than the range of effective temperature

reported in the literatures (Carnevale et al. 2014; Wang and Li 2012).

3.7 Effect of temperature on the PV panel power

A plot (Fig. 7) of the various PV panel powers versus operating temperature of the PV panel yielding the graphs of nonlinear function reveals the primary effect of temperature on the maximum value of each PV panel power

varied largely depending on the rate of water flow. The results (Fig. 7a–e) show that an increase in the temperature of PV panel led to an increased power of the PV panel which reaches a maximum value at around noontime (Gupta and Tiwari 2016; Kaldellis and Kokala 2010; Katz et al. 2001; Moharram et al. 2013). Figure 7a shows that the maximum solar power inputs of 294.0, 304.3 and 338.3 W reached at the temperatures of 46.8, 44.9 and 44.9 °C can be obtained from the panel of PV cooled by the water flow rates of 12, 18 and 24 L h⁻¹, respectively. This indicates that the maximum solar power input increases by 3.5% and 15.1% with an increase in the water flow rate by 50% from 12 to 18 L h⁻¹ and by 100% from 12 to 24 L h⁻¹, respectively. Figure 7b shows that the PV panel can generate the maximum electrical power outputs of 54.9, 52.7 and 62.2 W observed at the temperatures of 46.8, 44.9 and 44.9 °C when cooled with the water flow rates of 12, 18 and 24 L h⁻¹, respectively. The maximum electrical power output of having an irregular pattern depends on the behaviour of water flow. Figure 7c shows that the maximum thermal power outputs of 174.2, 188.2 and 181.1 W observed at the temperatures of 47.2, 44.9 and 44.9 °C can be harvested from the panel of PV cooled by the water flow rates of 12, 18 and 24 L h⁻¹, respectively. The maximum thermal power output has an irregular pattern with the highest value observed from the panel of PV cooled with a water flow rate of 18 L h⁻¹. Figure 7d shows that the maximum power losses of 65.6, 67.8 and 95.0 W observed from the panel of PV cooled by the water flow rates of 12, 18 and 24 L h⁻¹ occur at the temperatures of 46.8, 44.1 and 44.9 °C, respectively. In spite of the power losses of 65.6, 67.8 W which are almost similar to each other, the panel of PV cooled by a water flow rate of 24 L h⁻¹ has a power loss of 95.0 W and is more 40.1% higher than that cooled by the water flow rates of 12 and 18 L h⁻¹ (see Fig. 7d). Figure 7e shows the maximum overall power outputs of 228.4, 240.9 and 243.2 W observed from the panel of PV cooled by the water flow rates of 12, 18 and 24 L h⁻¹ could be occurred at the temperatures of 46.8, 44.9 and 44.9 °C, respectively. A trend of the lines-(i, ii, iii) in Fig. 7c is quite similar to that in Fig. 7e due to the amount of thermal power output generated by the water-cooled PV panel which represents the most important fraction of overall power output. A decrease in the operating PV module temperature caused by a water flowing through the copper tubes can lead to an increased efficiency of the PV panel (Bahaidarah et al. 2013).

The maximum solar power inputs of 294.0, 304.3 and 338.3 W, the maximum electrical power outputs of 54.9, 52.7 and 62.2 W and the maximum overall power outputs of 228.4, 240.9 and 243.2 W were verified from the experiments of using the panel of PV cooled by the water

flow rates of 12, 18 and 24 L h⁻¹ occurred at the temperatures of 46.8, 44.9 and 44.9 °C, respectively, around noontime of 11:35 (see Fig. 7a, b, e). The maximum thermal power outputs of 174.2, 188.2 and 181.1 W obtained from the experiments of using the panel of PV cooled by the water flow rates of 12, 18 and 24 L h⁻¹ observed at the temperatures of 47.2, 44.9 and 44.9 °C can occur at 12:05, 11:35 and 11:35 h, respectively, of the experimental day (see Fig. 7c). Meanwhile the operating temperatures of 47.2, 44.9 and 44.9 °C are all the highest temperature recorded during the experiments of using the PV panel cooled by the water flow rates of 12, 18 and 24 L h⁻¹, respectively. The maximum power losses of 65.6, 67.8 and 95.0 W obtained from the experiments of using the panel of PV cooled with the water flow rates of 12, 18 and 24 L h⁻¹ observed at the temperatures of 46.8, 44.1 and 44.9 °C can occur at 11:35, 12:35 and 11:35 h, respectively, of the experimental day (see Fig. 7d). In a previous study, it has been reported that the energy management algorithm of considering an electrical power output of the PV panel and the power losses of conduction and ventilation through buildings can reduce the energy consumption of space-heating loads to achieve energy savings (Al Essa 2021). Experimental evidence (Fig. 7) shows that all trendlines in the curves of plotting the various PV panel powers versus temperature provide (1) the maximum value of each PV panel power occurred around noontime and (2) the same value of each PV panel power probably recorded at two different temperatures. Applicability of the result findings is intertwined with an effective management of either electrical power, thermal power or power loss, optimised by choosing the proper cooling water flow rate. This provides the insights on the application of PV panel in the management of solar energy in the future.

4 Conclusions

The use of the quadratic equations has been proved able to predict the distributions of solar irradiation, power input, temperature, electrical power, thermal power, and power loss based on the empirical data monitored from the water-cooled and standard photovoltaic panels during the 6-h of the experimental period from 9:00 to 15:00 h. The correlation between two variables either electrical power and solar power input, thermal power and solar power input, power loss and solar power input or overall power output and solar power input can be understood from the linear regression analysis. The key results of this study are that (1) the amount and distribution of the solar power input, electrical power, thermal power, and power loss are dependent on both the solar irradiation received by a photovoltaic panel and the cooling water flow rate, (2) an

amount of solar power input determines the amount of various photovoltaic panel powers, while the rate of cooling water flowing through the copper tubes can affect the characteristics of photovoltaic panel power, (3) the amount and characteristics of additional electrical power generated by a water-cooled photovoltaic panel depend on the flow rate of cooling water passed through the copper tubes and the solar irradiation received by a photovoltaic panel surface, and (4) the maximum photovoltaic panel power reached around noontime can be recorded at two different operating temperatures observed from each cooling water flow rate, while the power loss in photovoltaic panel is very sensitive to the change of cooling water flow rate. The findings of this study will contribute to the logic of advanced integration in the management of photovoltaic panel, which offers an affordable access for the commercial and residential uses, while the service life of photovoltaic cells is maintained longer in the installation.

Acknowledgements The authors gratefully acknowledge the staffs at the Thermal Engineering Laboratory of Politeknik Negeri Jakarta for their contribution to assist the researchers to obtain the valuable data recorded from the pilot scale water-cooled PV panel and standard PV panel.

Authors' contributions All authors contributed extensively to the work presented in this paper. BB and RS conceived and designed the study and are the principal investigators. BB, MAF, MR and RS compiled and analysed the data and wrote the manuscript. BB, MAF, MR and RS analysed the data and contributed to discussion and made interpretation of mechanistic study data. MAF edited and finalised the manuscript. All authors critically reviewed and revised the manuscript, and they have read and approved the final version.

Funding This work was supported by the Ministry of Research, Technology and Higher, Indonesia for the Applied Research and Product Development (Penelitian Produk Terapan, PPT) No. 025/SP2H/LT/DRPM/IV/2017. All the funding bodies have no role in the design of the study and collection, analysis, and interpretation of data and in writing this manuscript.

Availability of data and materials The authors confirm that the data supporting the findings of this study are available within the article.

Declarations

Conflict of interest The authors declare that there is no potential conflict of interest associated with this manuscript.

References

- Abidi S, Sammouda H, Bennacer R (2014) Numerical analysis of three coolants heat exchanger associated to hybrid photovoltaic/thermal solar sensor. *Int J Energy Eng* 4:45–53. <https://doi.org/10.5923/j.ijee.20140403.01>
- Al Essa MJM (2021) Energy management of space-heating systems and grid-connected batteries in smart homes. *Energy Ecol Environ*. <https://doi.org/10.1007/s40974-021-00219-0>
- Alibabaei F, Saebnoori E, Fulazzaky MA, Talaeikhozani A, Roohi P, Moghadas F, Abdullah NH, Alian T (2021) An evaluation of the efficiency of odorant removal by sodium ferrate(VI) oxidation. *Measurement* 179:109488. <https://doi.org/10.1016/j.measurement.2021.109488>
- Allouhi A, Kousksou T, Jamil A, Zeraoui Y (2014) Modeling of a thermal adsorber powered by solar energy for refrigeration applications. *Energy* 75:589–596. <https://doi.org/10.1016/j.energy.2014.08.022>
- Alshuraiaan B (2021) Evaluation of the thermal performance of various nanofluids used to harvest solar energy. *Energy Ecol Environ*. <https://doi.org/10.1007/s40974-021-00213-6>
- Ando Y, Oku T, Yasuda M, Ushijima K, Matsuo H, Murozono M (2020) Dependence of electric power flow on solar radiation power in compact photovoltaic system containing SiC-based inverter with spherical Si solar cells. *Heliyon* 6:e03094. <https://doi.org/10.1016/j.heliyon.2019.e03094>
- Apostolaki-Iosifidou E, Codani P, Kempton W (2017) Measurement of power loss during electric vehicle charging and discharging. *Energy* 127:730–742. <https://doi.org/10.1016/j.energy.2017.03.015>
- Attia AAA, El-Assal BTA (2012) Experimental investigation of vapor chamber with different working fluids at different charge ratios. *Ain Shams Eng J* 3:289–297. <https://doi.org/10.1016/j.asej.2012.02.003>
- Avezov RR, Akhatov JS, Avezova NR (2011) A review on photovoltaic-thermal (PV-T) air and water collectors. *Appl Sol Energy* 47:169–183. <https://doi.org/10.3103/S0003701X11030042>
- Bahaidarah H, Subhan A, Gandhidasan P, Rehman S (2013) Performance evaluation of a PV (photovoltaic) module by back surface water cooling for hot climatic conditions. *Energy* 59:445–453. <https://doi.org/10.1016/j.energy.2013.07.050>
- Bangura AF, Xu X, Wakeham N, Peng N, Horii S, Hussey NE (2013) The Wiedemann-Franz law in the putative one-dimensional metallic phase of $\text{PrBa}_2\text{Cu}_4\text{O}_8$. *Sci Rep* 3:3261. <https://doi.org/10.1038/srep03261>
- Bouzidi B, Campana PE (2021) Optimization of photovoltaic water pumping systems for date palm irrigation in the Saharan regions of Algeria: increasing economic viability with multiple-crop irrigation. *Energy Ecol Environ*. <https://doi.org/10.1007/s40974-020-00195-x>
- Carnevale E, Lombardi L, Zanchi L (2014) Life cycle assessment of solar energy systems: comparison of photovoltaic and water thermal heater at domestic scale. *Energy* 77:434–446. <https://doi.org/10.1016/j.energy.2014.09.028>
- Chaplin DM, Fuller CS, Pearson GL (1954) A new silicon p-n junction photocell for converting solar radiation into electrical power. *J Appl Phys* 25:676–677. <https://doi.org/10.1063/1.1721711>
- Chen H, Riffat SB (2011) Development of photovoltaic thermal technology in recent years: a review. *Int J Low-Carbon Technol* 6:1–13. <https://doi.org/10.1093/ijlct/ctq042>
- Chen HY, Hou J, Zhang S, Liang Y, Yang G, Yang Y, Yu L, Wu Y, Li G (2009) Polymer solar cells with enhanced open-circuit voltage and efficiency. *Nat Photonics* 3:649–653. <https://doi.org/10.1038/nphoton.2009.192>
- Coskun C, Oktay Z, Dincer I (2011) Estimation of monthly solar radiation distribution for solar energy system analysis. *Energy* 36:1319–1323. <https://doi.org/10.1016/j.energy.2010.11.009>
- Daghighi R, Ibrahim A, Jin GL, Ruslan MH, Sopian K (2011) Predicting the performance of amorphous and crystalline silicon based photovoltaic solar thermal collectors. *Energy Convers Manag* 52:1741–1747. <https://doi.org/10.1016/j.enconman.2010.10.039>

- Daut I, Zainuddin F, Irwan YM, Razliana ARN (2012) Analysis of solar irradiance and solar energy in Perlis, Northern of Peninsular Malaysia. *Energy Procedia* 18:1421–1427. <https://doi.org/10.1016/j.egypro.2012.05.158>
- Dubey S, Tiwari GN (2009) Analysis of PV/T flat plate water collectors connected in series. *Sol Energy* 83:1485–1498. <https://doi.org/10.1016/j.solener.2009.04.002>
- Dubey S, Sandhu GS, Tiwari GN (2009) Analytical expression for electrical efficiency of PV/T hybrid air collector. *Appl Energy* 86:697–705. <https://doi.org/10.1016/j.apenergy.2008.09.003>
- Dubey S, Sarvaiya JN, Seshadri B (2013) Temperature dependent photovoltaic (PV) efficiency and its effect on PV production in the world—a review. *Energy Procedia* 33:311–321. <https://doi.org/10.1016/j.egypro.2013.05.072>
- Fang G, Hu H, Liu X (2010) Experimental investigation on the photovoltaic-thermal solar heat pump air-conditioning system on water-heating mode. *Exp Therm Fluid Sci* 34:736–743. <https://doi.org/10.1016/j.expthermflusci.2010.01.002>
- Fulazzaky MA (2011) Determining the resistance of mass transfer for adsorption of the surfactants onto granular activated carbons from hydrodynamic column. *Chem Eng J* 166:832–840. <https://doi.org/10.1016/j.cej.2010.11.052>
- Fulazzaky T, Fulazzaky MA (2019) Using the fasting blood sugar and glycated haemoglobin models for predicting the personal management of type-2 diabetes. *Eur J Med Health Sci* 1:5. <https://doi.org/10.24018/ejmed.20>
- Fulazzaky MA, Omar R (2012) Removal of oil and grease contamination from stream water using the granular activated carbon black filter. *Clean Technol Environ Policy* 14:965–971. <https://doi.org/10.1007/s10098-012-0471-8>
- Gupta N, Tiwari GN (2016) Review of passive heating/cooling systems of buildings. *Energy Sci Eng* 4:305–333. <https://doi.org/10.1002/ese3.129>
- Herrando M, Markides CN (2016) Hybrid PV and solar-thermal systems for domestic heat and power provision in the UK: Techno-economic considerations. *Appl Energy* 161:512–532. <https://doi.org/10.1016/j.apenergy.2015.09.025>
- Hove T (2000) A method for predicting long-term average performance of photovoltaic systems. *Renew Energy* 21:207–229. [https://doi.org/10.1016/S0960-1481\(99\)00131-7](https://doi.org/10.1016/S0960-1481(99)00131-7)
- Ibn-Mohammed T, Koh SCL, Reaney IM, Acquaye A, Schileo G, Mustapha KB, Greenough R (2017) Perovskite solar cells: an integrated hybrid lifecycle assessment and review in comparison with other photovoltaic technologies. *Renew Sustain Energy Rev* 80:1321–1344. <https://doi.org/10.1016/j.rser.2017.05.095>
- Idoko L, Anaya-Lara O, McDonald A (2018) Enhancing PV modules efficiency and power output using multi-concept cooling technique. *Energy Rep* 4:357–369. <https://doi.org/10.1016/j.egypr.2018.05.004>
- Irvine S (2017) Solar cells and photovoltaics. In: Kasap S, Capper P (eds) *Springer handbook of electronic and photonic materials*. Springer handbooks. Springer, Cham
- Jamar A, Majid ZAA, Azmi WH, Norhafana M, Razak AA (2016) A review of water heating system for solar energy applications. *Int Commun Heat Mass Transf* 76:178–187. <https://doi.org/10.1016/j.icheatmasstransfer.2016.05.028>
- Ji J, Han J, Chow T, Yi H, Lu J, He W, Sun W (2006) Effect of fluid flow and packing factor on energy performance of a wall-mounted hybrid photovoltaic/water-heating collector system. *Energy Build* 38:1380–1387. <https://doi.org/10.1016/j.enbuild.2006.02.010>
- Jones AD, Underwood CP (2002) A modelling method for building-integrated photovoltaic power supply. *Build Serv Eng Res Technol* 23:167–177. <https://doi.org/10.1191/0143624402bt0400a>
- Joshi AS, Tiwari A, Tiwari GN, Dincer I, Reddy BV (2009) Performance evaluation of a hybrid photovoltaic thermal (PV/T) (glass-to-glass) system. *Int J Therm Sci* 48:154–164. <https://doi.org/10.1016/j.ijthermalsci.2008.05.001>
- Kaldellis JK, Kokala A (2010) Quantifying the decrease of the photovoltaic panels' energy yield due to phenomena of natural air pollution disposal. *Energy* 35:4862–4869. <https://doi.org/10.1016/j.energy.2010.09.002>
- Kalogirou SA, Tripanagnostopoulos Y (2006) Hybrid PV/T solar systems for domestic hot water and electricity production. *Energy Convers Manag* 47:3368–3382. <https://doi.org/10.1016/j.enconman.2006.01.012>
- Katz EA, Faiman D, Tuladhar SM, Kroon JM, Wienk MM (2001) Temperature dependence for the photovoltaic device parameters of polymer-fullerene solar cells under operating conditions. *J Appl Phys* 90:5343–5350. <https://doi.org/10.1063/1.1412270>
- Khordehgah N, Zabnienska-Góra A, Jouhara H (2020) Energy performance analysis of a PV/T system coupled with domestic hot water system. *ChemEngineering* 4:22. <https://doi.org/10.3390/chemengineering4020022>
- Kostic LT, Pavlovic TM, Pavlovic ZT (2010) Influence of reflectance from flat aluminum concentrators on energy efficiency of PV/Thermal collector. *Appl Energy* 87:410–416. <https://doi.org/10.1016/j.apenergy.2009.05.038>
- Kumar S, Tiwari A (2010) Design, fabrication and performance of a hybrid photovoltaic/thermal (PV/T) active solar still. *Energy Convers Manag* 51:1219–1229. <https://doi.org/10.1016/j.enconman.2009.12.033>
- Li M, Wang RZ, Luo HL, Wang LL, Huang HB (2002) Experiments of a solar flat plate hybrid system with heating and cooling. *Appl Therm Eng* 22:1445–1454. [https://doi.org/10.1016/S1359-4311\(02\)00067-4](https://doi.org/10.1016/S1359-4311(02)00067-4)
- Li M, Li GL, Ji X, Yin F, Xu L (2011) The performance analysis of the trough concentrating solar photovoltaic/thermal system. *Energy Convers Manag* 52:2378–2383. <https://doi.org/10.1016/j.enconman.2010.12.039>
- Lin H, Xu S, Zhang YQ, Wang X (2014) Electron transport and bulk-like behavior of Wiedemann-Franz law for sub-7 nm-thin iridium films on silkworm silk. *ACS Appl Mater Interface* 6:11341–11347. <https://doi.org/10.1021/am501876d>
- Maghami MR, Hizam H, Gomes C, Radzi MA, Rezadad MI, Hajighorbani S (2016) Power loss due to soiling on solar panel: a review. *Renew Sustain Energy Rev* 59:1307–1316. <https://doi.org/10.1016/j.rser.2016.01.044>
- Moharram KA, Abd-Elhady MS, Kandil HA, El-Sherif H (2013) Enhancing the performance of photovoltaic panels by water cooling. *Ain Shams Eng J* 4:869–877. <https://doi.org/10.1016/j.asej.2013.03.005>
- Mondol JD, Yohanis YG, Smyth M, Norton B (2005) Long-term validated simulation of a building integrated photovoltaic system. *Sol Energy* 78:163–176. <https://doi.org/10.1016/j.solener.2004.04.021>
- Mortezapour H, Ghobadian B, Khoshtaghaza MH, Minaei S (2012) Performance analysis of a two-way hybrid photovoltaic/thermal solar collector. *J Agric Sci Technol* 14:767–780
- Nateqi M, Rajabi Zargarabadi M, Rafee R (2021) Experimental investigations of spray flow rate and angle in enhancing the performance of PV panels by steady and pulsating water spray system. *SN Appl Sci* 3:130. <https://doi.org/10.1007/s42452-021-04169-4>
- Nguyen KB, Yoon SH, Choi JH (2012) Effect of working-fluid filling ratio and cooling-water flow rate on the performance of solar collector with closed-loop oscillating heat pipe. *J Mech Sci Technol* 26:251–258. <https://doi.org/10.1007/s12206-011-1005-8>

- Ostertagová E (2012) Modelling using polynomial regression. *Procedia Eng* 48:500–506. <https://doi.org/10.1016/j.proeng.2012.09.545>
- Pratiwi S, Juerges N (2020) Review of the impact of renewable energy development on the environment and nature conservation in Southeast Asia. *Energy Ecol Environ* 5:221–239. <https://doi.org/10.1007/s40974-020-00166-2>
- Ratlamwala TAH, Gadalla MA, Dincer I (2011) Performance assessment of an integrated PV/T and triple effect cooling system for hydrogen and cooling production. *Int J Hydrogen Energy* 36:11282–11291. <https://doi.org/10.1016/j.ijhydene.2010.11.121>
- Saksono T, Fulazzaky MA (2020) Predicting the accurate period of true dawn using a third-degree polynomial model. *NRIAG J Astron Geophys* 9:238–244. <https://doi.org/10.1080/20909977.2020.1738106>
- Salabaş EL, Salabaş A, Mereu B, Caglar O, Kupich M, Cashmore JS, Sinicco I (2016) Record amorphous silicon single-junction photovoltaic module with 9.1% stabilized conversion efficiency on 1.43 m². *Prog Photovolt* 24:1068–1074. <https://doi.org/10.1002/pip.2760>
- Sarhaddi F, Farahat S, Ajam H, Behzadmehr A (2010) Exergetic performance assessment of a solar photovoltaic thermal (PV/T) air collector. *Energy Build* 42:2184–2199. <https://doi.org/10.1016/j.enbuild.2010.07.011>
- Schmidt M, Astrouski I, Reppich M, Raudensky M (2016) Solar panel cooling system with hollow fibres. *Appl Sol Energy* 52:86–92. <https://doi.org/10.3103/S0003701X16020213>
- Schneider A, Hommel G, Blettner M (2010) Linear regression analysis. *Dtsch Arztebl Int* 107:776–782. <https://doi.org/10.3238/arztebl.2010.0776>
- Shahsavari A, Ameri M (2010) Experimental investigation and modeling of a direct-coupled PV/T air collector. *Sol Energy* 84:1938–1958. <https://doi.org/10.1016/j.solener.2010.07.010>
- Skoplaki E, Palyvos JA (2009) Operating temperature of photovoltaic modules: a survey of pertinent correlations. *Renew Energy* 34:23–29. <https://doi.org/10.1016/j.renene.2008.04.009>
- Smolen T, Chuderski A (2015) The quadratic relationship between difficulty of intelligence test items and their correlations with working memory. *Front Psychol* 6:1270. <https://doi.org/10.3389/fpsyg.2015.01270>
- Tonui JK, Tripanagnostopoulos Y (2008) Performance improvement of PV/T solar collectors with natural air flow operation. *Sol Energy* 82:1–12. <https://doi.org/10.1016/j.solener.2007.06.004>
- Tyagi VV, Kaushik SC, Tyagi SK (2012) Advancement in solar photovoltaic/thermal (PV/T) hybrid collector technology. *Renew Sustain Energy Rev* 16:1383–1398. <https://doi.org/10.1016/j.rser.2011.12.013>
- Wang ZW, Li SS (2012) Lattice relaxation of graphene under high magnetic field. *J Phys Condens Matter* 24:265302. <https://doi.org/10.1088/0953-8984/24/26/265302>
- Wang H, Liu J, Zhang X, Takahashi K (2013) Breakdown of Wiedemann-Franz law in individual suspended polycrystalline gold nanofilms down to 3 K. *Int J Heat Mass Transf* 66:585–591. <https://doi.org/10.1016/j.ijheatmasstransfer.2013.07.066>
- Zhao J, Song Y, Lam WH, Liu W, Liu Y, Zhang Y, Wang DY (2011) Solar radiation transfer and performance analysis of an optimum photovoltaic/thermal system. *Energy Convers Manag* 52:1343–1353. <https://doi.org/10.1016/j.enconman.2010.09.032>
- Zhou W, Yang H, Fang Z (2007) A novel model for photovoltaic array performance prediction. *Appl Energy* 84:1187–1198. <https://doi.org/10.1016/j.apenergy.2007.04.006>
- Zimmermann S, Meijer I, Tiwari MK, Paredes S, Michel B, Poulikakos D (2012) Aquasar: a hot water cooled data center with direct energy reuse. *Energy* 43:237–245. <https://doi.org/10.1016/j.energy.2012.04.037>